

A Pharmacological Chaperone Therapy for Acute Intermittent Porphyrria

Helene J. Bustad,¹ Karen Toska,² Caroline Schmitt,^{3,4} Marta Vorland,² Lars Skjærven,¹ Juha P. Kallio,¹ Sylvie Simonin,^{3,4} Philippe Letteron,⁴ Jarl Underhaug,⁵ Sverre Sandberg,^{2,6,7} and Aurora Martinez¹

¹Department of Biomedicine, University of Bergen, 5020 Bergen, Norway; ²Norwegian Porphyrria Centre (NAPOS), Laboratory for Clinical Biochemistry, Haukeland University Hospital, 5021 Bergen, Norway; ³Assistance Publique Hôpitaux de Paris (AP-HP), Centre Français des Porphyrries, Hôpital Louis Mourier, 92700 Colombes, France; ⁴INSERM U1149, Center for Research on Inflammation (CRI), Université de Paris, 75018 Paris, France; ⁵Department of Chemistry, University of Bergen, 5020 Bergen, Norway; ⁶Department of Global Public Health and Primary Care, University of Bergen, 5020 Bergen, Norway; ⁷The Norwegian Quality Improvement of Primary Care Laboratories, Haralds plass Deaconess Hospital, 5009 Bergen, Norway

Mutations in hydroxymethylbilane synthase (HMBS) cause acute intermittent porphyria (AIP), an autosomal dominant disease where typically only one HMBS allele is mutated. In AIP, the accumulation of porphyrin precursors triggers life-threatening neurovisceral attacks and at long-term, entails an increased risk of hepatocellular carcinoma, kidney failure, and hypertension. Today, the only cure is liver transplantation, and a need for effective mechanism-based therapies, such as pharmacological chaperones, is prevailing. These are small molecules that specifically stabilize a target protein. They may be developed into an oral treatment, which could work curatively during acute attacks, but also prophylactically in asymptomatic HMBS mutant carriers. With the use of a 10,000 compound library, we identified four binders that further increased the initially very high thermal stability of wild-type HMBS and protected the enzyme from trypsin digestion. The best hit and a selected analog increased steady-state levels and total HMBS activity in human hepatoma cells over-expressing HMBS, and in an *Hmbs*-deficient mouse model with a low-expressed wild-type-like allele, compared to untreated controls. Moreover, the concentration of porphyrin precursors decreased in liver of mice treated with the best hit. Our findings demonstrate the great potential of these hits for the development of a pharmacological chaperone-based corrective treatment of AIP by enhancing wild-type HMBS function independently of the patients' specific mutation.

drate intake, alcohol, or porphyrinogenic drugs, activate the expression of hepatic δ -aminolevulinic acid (ALA) synthase 1 (ALAS1). Elevated levels of ALAS1, together with diminished HMBS activity, lead to accumulation of the heme precursors ALA and porphobilinogen (PBG). PBG and in particular ALA are believed to be toxic metabolites related to the neuropathy of the disease and to trigger the acute attacks.⁵ In addition, PBG at high concentrations may further decrease HMBS activity.^{6,7} The attacks are unspecific with common symptoms, such as abdominal pain, nausea, tachycardia, and hypertension, in addition to various neurological and psychiatric symptoms.¹ More severe symptoms, such as acute psychosis and potentially life-threatening symptoms—paralysis and coma—may also occur.^{8,9} AIP patients have a higher risk of developing hepatocellular carcinoma, hypertension, and kidney failure.^{10,11}

Intravenous administration of human hemin is the established specific treatment for severe and recurrent AIP attacks, providing exogenous heme that downregulates ALAS1 expression.¹² However, repeated therapy can be associated with reduced efficacy² but may also give a chronic activation of heme oxygenase 1 expression that will trigger ALAS1 and subsequently recurrent attacks.¹³ Liver transplantation is today the only curative alternative for chronically ill patients.¹⁴ Although several therapeutic options are under investigation,^{15–18} there is still a need for effective mechanism-based pharmacotherapies, as this would provide a noninvasive, oral treatment that could possibly work prophylactically,¹⁹ as well as a specific medication during an acute attack.

Pharmacological chaperones (PCs) are defined as small molecular weight compounds that specifically target and interact with unstable and incorrectly folded proteins. PC binding stabilizes the target protein, protecting it from early degradation, thus increasing its half-life

INTRODUCTION

Acute intermittent porphyria (AIP; OMIM: 176000) is an inborn error of metabolism caused by mutations in the third enzyme of the heme synthesis pathway, i.e., hydroxymethylbilane synthase (HMBS; EC 2.5.1.61). To date, more than 420 different mutations in the *HMBS* gene have been reported (available at <http://www.hgmd.cf.ac.uk/ac/gene.php?gene=HMBS>), including both catalytically and/or conformationally deleterious mutations. The prevalence of AIP is about 1 in 20,000–100,000, depending on the ethnic group.^{1,2} However, the overall penetrance is 0.5%–1% in the general population and 10%–20% within families.^{3,4} Factors, such as hormonal changes, low carbohy-

Received 6 January 2019; accepted 11 November 2019;
<https://doi.org/10.1016/j.ymthe.2019.11.010>

Correspondence: Aurora Martinez, Department of Biomedicine, University of Bergen, Jonas Lies vei 91, 5020 Bergen, Norway.

E-mail: aurora.martinez@uib.no



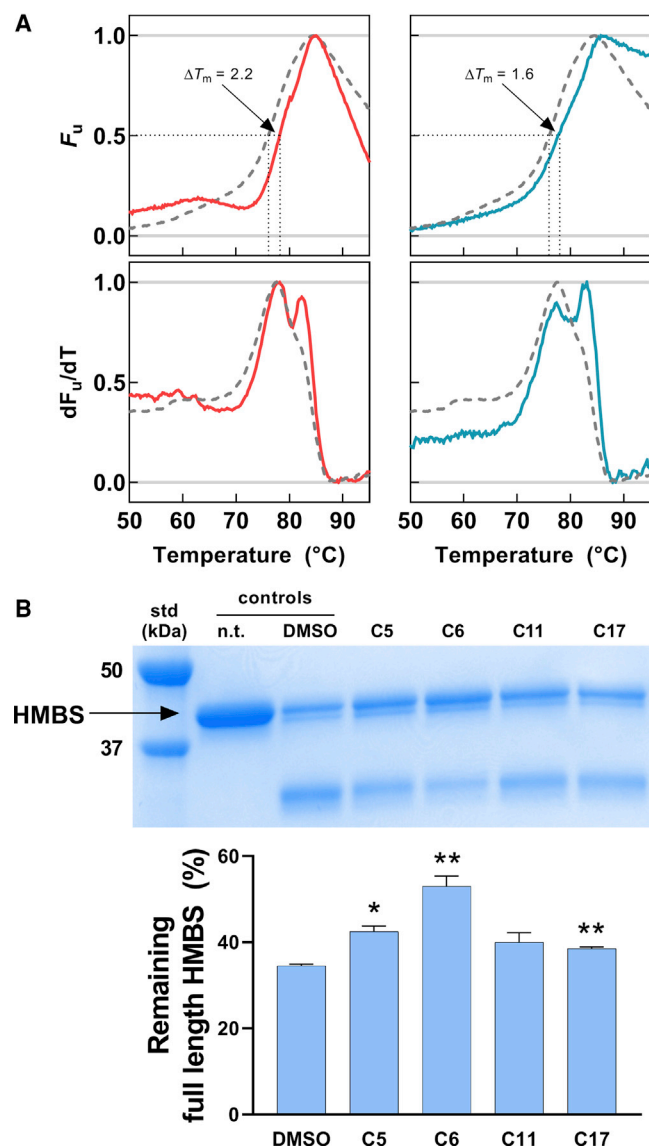


Figure 1. Screening and Validation of Stabilizing Hit Compounds for HMBS

(A) Representative differential scanning fluorimetry (DSF) profiles for HMBS in the absence and presence of hit compounds. The thermal upshift values (ΔT_m) for the compounds are determined from the midpoint denaturation temperatures (T_m at $y = 0.5$) compared to the control sample with 2% DMSO ($T_m = 76.6 \pm 0.5^\circ\text{C}$). The profiles represent recombinant WT-HMBS incubated with the 0.04-mg/mL compound (average concentration 122 μM) in 2% DMSO (red; C5; blue; C6; see the formulas in Table 2) and the control sample without compound, with 2% DMSO (dotted gray). (B) Protection of hit compounds against limited tryptic proteolysis of WT-HMBS. Top: SDS-PAGE showing the effect of the indicated compounds (84 μM and 2% DMSO) on HMBS trypsinolysis. std, low molecular weight standards; control n.t., no trypsin added; control DMSO, HMBS with 2% DMSO and trypsin. Bottom: quantification of the lowest 31.5-kDa band relative to the full-length HMBS at 42.5 kDa. * $p < 0.05$ and ** $p < 0.01$ for differences compared to the DMSO control, calculated by unpaired two-tailed t test. Data are presented as mean \pm SD.

and enhancing its cellular activity.^{20–22} PC therapy has been demonstrated as a potential treatment for protein misfolding diseases, such as cystic fibrosis,²³ phenylketonuria,²⁴ lysosomal storage disorders,²⁵ and congenital erythropoietic porphyria.²⁶ Residual enzymatic activity is required for the PCs to enhance the activity of conformational mutations that result in an unstable and misfolded enzyme. The focus for the PC discovery in the above-mentioned recessive genetic diseases has been the development of PCs targeting either one particularly common mutation in the target protein²³ or a range of responsive mutations.²⁵ However, AIP presents as a model disorder for autosomal dominantly inherited diseases, where fully functional wild-type (WT) HMBS is expressed from only one allele and provides $\sim 50\%$ of normal enzymatic activity. This is seemingly enough to maintain normal cellular metabolism,²⁷ although once the heme synthesis is challenged, the amount of functional gene product is unable to compensate for the allele that holds the HMBS mutation. Relevantly for AIP and other inherited disorders with haploinsufficiency, PCs have demonstrated value in increasing the stability of WT enzymes *in vitro* and *in vivo*.^{24,28–30} In the case of AIP, however, possible porphyrinogenicity of a future drug must also be taken into account, as the list of drugs that may cause an acute crisis is very large.^{31,32}

In this work, we present the discovery and identification of potential PCs to treat AIP. We have focused on the effect of candidate molecules selected by high-throughput screening and validated *in vitro* by analyzing their effect on the conformational and kinetic stability of purified recombinant WT-HMBS. Furthermore, we evaluated their PC potential in human hepatoma HepG2 cells overexpressing WT-HMBS and *in vivo* using an *Hmbs*-deficient T1/T2^{-/-} mouse model. The *Hmbs*-deficient mice exhibit $\sim 30\%$ of normal hepatic activity and is compound heterozygous of one null allele and one low-expressed normal allele.³³ Our findings reveal hit compounds that stabilize WT-HMBS and show a large potential in the development of a PC therapy for AIP, independent of the patients' mutation, with the possibility of being both curative for acute attacks and having a prophylactic effect to impede recurrent acute attacks.

RESULTS

Selection of Potential Pharmacological Chaperones

The effect of 10,000 compounds on the thermostability of recombinant WT-HMBS was investigated using differential scanning fluorimetry (DSF). The thermal melting profile of HMBS, studied by DSF and other methods, shows a major transition with a half-denaturation temperature (T_m) of $\sim 74^\circ\text{C}$,³⁴ which is slightly increased in the presence of 2% DMSO ($T_m = 76.6 \pm 0.5^\circ\text{C}$) (Figure 1A, gray dotted line). This value, where the temperature of the normalized fluorescence curves crossed $y = 0.5$, was used as a reference to determine the shifts in T_m in the presence of compound compared to the DMSO control ($\Delta T_m = T_m(\text{compound hit}) - T_m(\text{DMSO control})$). Positive shifts indicate ligand binding and protein stabilization.³⁵ The first derivative (dF/dT ; Figure 1A, bottom) was used for visualization of the complexity and qualitative inspection of the transitions. Despite the remarkable conformational stability of HMBS, which

Table 1. Primary Hit Compounds

Compound ID	ΔT_m^a (°C)	Relative Activity, Standard ^b	Relative Activity, Pre-Incubated at 70°C ^c	Protection against Tryptic Proteolysis ^d
Control	–	1.00	1.00	–
C4	1.6	1.04 ± 0.05	0.92 ± 0.07**	ND
C5 ^e	2.1	1.05 ± 0.02	1.04 ± 0.05	+*
C6 ^e	1.6	0.98 ± 0.06	1.01 ± 0.06	++**
C8	4.5	1.01 ± 0.03	0.92 ± 0.05**	ND
C9	3.8	0.98 ± 0.03	1.04 ± 0.07	+/-
C11 ^e	1.6	1.00 ± 0.03	1.01 ± 0.04	+
C12	2.2	1.07 ± 0.05	0.94 ± 0.09	+/-
C15	1.5	1.00 ± 0.02	0.91 ± 0.07*	ND
C16	2.0	1.04 ± 0.04	0.91 ± 0.03***	ND
C17 ^e	2.3	1.09 ± 0.05	1.07 ± 0.04	+*
C19	2.0	1.04 ± 0.02	0.95 ± 0.06	+/-
C23	1.6	0.92 ± 0.05**	0.96 ± 0.06*	ND
C24	2.3	1.08 ± 0.03	0.81 ± 0.06****	ND

The effect of the 13 primary hit compounds on the T_m of HMBS measured by DSF, enzymatic activity, and limited tryptic proteolysis of the enzyme. * $p < 0.05$, ** $p < 0.01$, *** $p < 0.001$, and **** $p < 0.0001$ for significance compared with the DMSO control sample, calculated by unpaired two-tailed t test. Data are presented as mean ± SD.

^aThe thermal upshift values (ΔT_m) monitored by DSF. The average compound concentration in DSF screening was 122 μ M (2% DMSO).

^bActivity assay performed at standard conditions, with 100 μ M PBG at 37°C, 84 μ M compound, and 2% DMSO, which was added in all controls.

^cAssay, including preincubation of HMBS with compound at 70°C, and subsequent standard activity assay, with 100 μ M PBG at 37°C, 84 μ M compound, and 2% DMSO.

^d+/-, ±2%; +, >4%; ++, 10% remaining full-length HMBS relative to DMSO; ND, not determined; see main text and Figure 1B for details.

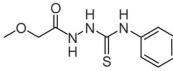
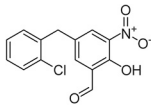
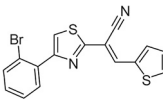
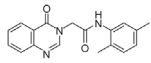
^eHit compounds selected for cell studies.

presents a significantly higher T_m than the customary value for the majority of mammalian proteins ($T_m \approx 55^\circ\text{C}$),³⁶ we discovered several compounds causing positive ΔT_m values. 64 compounds stabilized HMBS $\geq 1.5^\circ\text{C}$ at 0.04 mg/mL (80–167 μ M) (see Figure 1A for representative stabilizing compounds) and were further filtered against pan assay interference compounds.³⁷ The remaining 22 compounds were analyzed by concentration-dependent DSF, with concentrations up to 84–167 μ M, to corroborate specific binding (data not shown), and 13 compounds were assigned as primary hits and selected for further analyses (Tables 1 and S1). These compounds did not have a clear structural resemblance.

Validation of Hit Compounds

We investigated the effect of the 13-hit compounds on the enzyme activity and conformational stability of HMBS. HMBS activity of the recombinant enzyme was measured in the absence and presence of compounds (at 84 μ M) at standard conditions (37°C) and considering the high thermal stability of WT-HMBS, also after preincubation at 70°C for 20 min. The results are presented in Table 1. Compounds that displayed an inhibitory effect of 8%–20% at one or both conditions were eliminated, leaving seven noninhibitory poten-

Table 2. Hit Compounds Selected for Validation

ID	Structure	K_M (PBG) ^a (μ M)	V_{max}^a (nmol/min/mg)
Control	–	86 ± 5	61 ± 2
C5		81 ± 5	55 ± 1**
C6		69 ± 4*	56 ± 1*
C11		77 ± 5	59 ± 1
C17		81 ± 2	58 ± 2

Chemical structure of the four hit compounds selected for cellular studies and steady-state enzyme kinetic parameters of HMBS in the presence of the compounds. * $p < 0.05$ and ** $p < 0.01$ for significant difference compared with the values for the control sample (with 2% DMSO), calculated by unpaired two-tailed t test. Data are presented as mean ± SD.

^aEffect of the compounds on the enzyme kinetic parameters for HMBS activity, measured at fixed compound concentration (84 μ M in 2% DMSO) and variable PBG (0–1 mM) at 37°C, and fitted to Michaelis-Menten kinetics.

tial hits (compounds [C] 5, 6, 9, 11, 12, 17, and 19). To ensure a reliable selection of hit compounds for testing in cells and *in vivo*, limited tryptic proteolysis was applied to select the hit compounds with the greatest capacity to increase the conformational stability of HMBS. Proteolysis of WT-HMBS (DMSO control) provided three major bands with relative content 34.5 ± 0.3%, 14.7 ± 0.8%, and 50.9 ± 0.5% (mean ± SD) at the selected conditions, corresponding to remaining full-length HMBS (~42.5 kDa), and two fragments of ~41.0 kDa and ~31.5 kDa, respectively (Figure 1B). Protection against proteolysis was obtained for hit compounds C5, C6, C11, and C17, notably for C6, which provided a higher proportion of full-length HMBS after tryptic treatment compared with the DMSO control (Figure 1B). The chemical structures of these compounds are shown in Table 2, together with their effect (at 84 μ M) on the steady-state enzyme kinetic parameters of HMBS. A decreased V_{max} but a similar K_M (PBG) was obtained in the presence of C5, indicating a noncompetitive, inhibitory effect, but the effects of C6, which reduced both K_M and V_{max} , agreed with mixed/uncompetitive inhibition. Neither C11 nor C17 caused any changes in K_M or V_{max} . C5, C6, C11, and C17 were selected for further validation in cells.

The Effect of Hit Compounds in HepG2 Cells

The stabilizing and potential PC effect of the selected hit compounds C5, C6, C11, and C17 was investigated in HepG2 cells overexpressing HMBS by analyzing the steady-state levels of the enzyme as a function of compound concentration. Quantitative immunoblotting revealed an increasing amount of HMBS for C6 (Figure 2A) but not for C5, C11, and C17 (Figure S1). Moreover, the addition of C11 and C17 to HepG2 cells

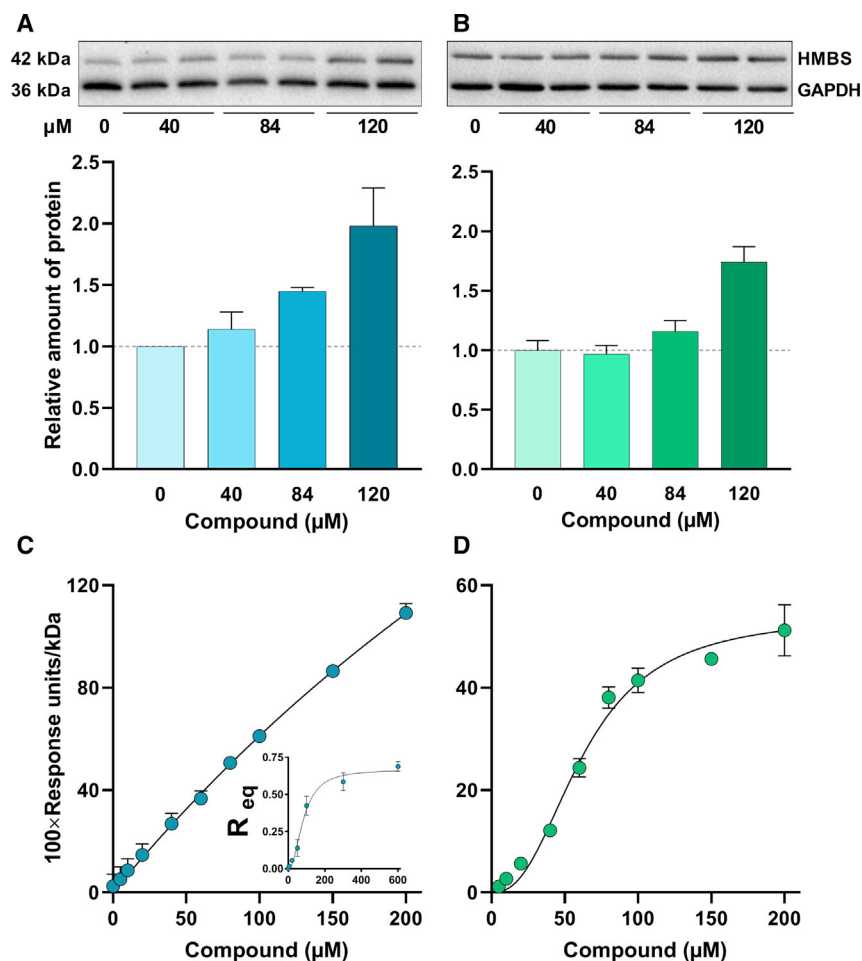


Figure 2. Effect of the Hit Compounds C6 and Its Analog C6-3 on HMBS in HepG2 Cells and Concentration-Dependent Surface Plasmon Resonance

(A and B) Western blotting and immunoquantification of the relative amount of HMBS in cell lysates from WT-HMBS stably transfected HepG2 cells treated with either C6 (A) or its analog C6-3 (B; see molecular structure in Table 3 and main text thereafter) at the indicated concentrations. DMSO (2%) was included in all samples. Representative blots are shown, and the histograms below represent the quantification of the relative HMBS levels ($n = 3$) using GAPDH as the protein loading control. Concentration-dependent binding of C6 (C) and C6-3 (D) to HMBS measured by SPR. The half-maximal binding ($S_{0.5}$) values were $83 \pm 7 \mu\text{M}$ for C6, obtained by subsequent Octet measurements (C, inset), and $63 \pm 3 \mu\text{M}$ for C6-3, obtained from the SPR binding isotherm (D). Data are presented as mean \pm SD.

seemed to have adverse effects, as we observed severe morphological changes and cell death already at low compound concentrations. These two compounds were therefore excluded from further studies.

The Initial Effect of Hit Compounds on ALA and PBG Excretion in *Hmbs*-Deficient Mice

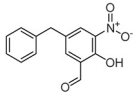
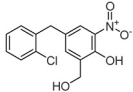
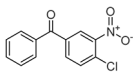
In view of the promising results with C6 (5-[(2-chlorophenyl)methyl]-2-hydroxy-3-nitrobenzaldehyde) as an HMBS stabilizer *in vitro* and in cells (Figures 1 and 2A; Table 1), we continued by testing its effect in a preliminary trial (Trial T1/T2-A) using the compound heterozygous *Hmbs*-deficient T1/T2^{-/-} mouse model for AIP. This model allows monitoring the increased level of precursors ALA and PBG in urine after phenobarbital induction, which stimulates the heme synthesis. C5 (2-methoxy-N-[(phenylcarbamothioyl)amino]acetamide) was also included in the trial due to its good stabilizing effect *in vitro* (Figure 1; Table 1). A schematic overview of the mice trials can be seen in Figure S2. In trial T1/T2-A, two groups of six mice each were given 10 mg/kg/day of either C5 or C6 for 12 days. A control group of six mice, treated with only DMSO, was also included. All mice were given phenobarbital (Gardenal) during the last 3 days of the study. No

apparent toxicity in the treated mice was detected, as assessed by normal health and behavior during the 12-day study and organ appearances after sacrifice. As previously reported, *Hmbs*-deficient T1/T2^{-/-} mice do not show elevated excretion of urinary ALA and PBG until induction of biochemical acute attacks,³³ and indeed a rapid increase in both urinary ALA and PBG was seen for the control mice by day 11 and even higher by day 12, following the phenobarbital administration (Figures S3A and S3B, gray bars). The treatment with 10 mg/kg/day did not cause any significant change in HMBS protein levels or activity in either erythrocytes or liver, compared to the non-treated *Hmbs*-deficient mice (data not shown). However, a decreasing tendency in urinary levels of ALA, but not PBG, was observed for both C6 and C5 treatment by day 12 (Figure S3B) compared to nontreated mice, suggesting that a higher compound concentration may result in an increased metabolite level correction. Similarly, compound analogs with higher affinity might increase the effect due to a more efficient dose-dependent effect *in vivo*.

Identification of Hit Compound Analogs

Through the implementation of a compound similarity search of the best hit C6, we aimed to identify analogs that corroborated or even improved the stabilizing effects on HMBS. We obtained three close analogs with a chemical similarity of >70% to the query C6, calculated using the Tanimoto coefficient for 2-dimensional (2D) similarity searching^{38,39} (Table 3). The analogs were tested on recombinant WT-HMBS using DSF and tryptic proteolysis, and analog C6-3 ((4-chloro-3-nitrophenyl)(phenyl)methanone) (Table 3) was selected for further studies. In cells, C6-3 increased the HMBS protein levels (Figure 2B), and enzyme kinetic analyses showed a weak noncompetitive inhibition (Table 3). C6-3 was therefore selected for further analysis.

Table 3. Compound Analogs of C6

ID	IUPAC Name and Structure	MW	ΔT_m^a (°C)	Protection against Tryptic Proteolysis ^b	K_M (PBG) ^c (μ M)	V_{max}^c (nmol/min/mg)
Control	–	–	–	–	86 ± 5	61 ± 2
C6-1	5-benzyl-2-hydroxy-3-nitrobenzaldehyde 	257.24	6.6	+/-	–	–
C6-2	4-[(2-chlorophenyl)methyl]-2-(hydroxymethyl)-6-nitrophenol 	293.7	4.7	+/-	–	–
C6-3	(4-chloro-3-nitrophenyl)(phenyl)methanone 	261.66	4.9	+	84 ± 8	$54 \pm 2^{**}$

The analogs of C6 were selected from the compound similarity search calculated using the Tanimoto coefficient. The Tanimoto coefficient is used to calculate the 2D similarity between sets of chemical structures.³⁸ The effect of the analogs on both the ΔT_m measured by DSF and on the limited tryptic proteolysis of HMBS was determined. Steady-state enzymatic kinetic parameters of HMBS in the presence of analogs were only determined for the analog that protected toward tryptic proteolysis (C6-3). * $p < 0.05$ and ** $p < 0.01$ for significant difference compared with the values for the control sample (with 2% DMSO), calculated by unpaired two-tailed t test. Data are presented as mean \pm SD. IUPAC, International Union of Pure and Applied Chemistry.

^aThe thermal upshift values (ΔT_m) monitored by DSF. The average compound concentration in DSF screening was 122 μ M (2% DMSO).

^b+/-, $\pm 2\%$; +, $>4\%$.

^cEffect of the compounds on the enzyme kinetic parameters for HMBS activity, measured at fixed compound concentration (84 μ M with 2% DMSO) and variable PBG (0–1 mM) at 37°C, and fitted to Michaelis-Menten kinetics.

The Binding of the Hit Compounds C6 and C6-3 to HMBS

The binding of C6 and C6-3 to HMBS was analyzed by surface plasmon resonance (SPR), measuring the response units from the compound concentration-dependent, steady-state binding response, and analyzed assuming a 1:1 binding model (Figures 2C and 2D). C6 showed some unspecific binding by SPR, and an accurate concentration of compound at half-maximal binding ($S_{0.5}$) could not be obtained (Figures 2C, S4A, and S4B). The binding of C6 to HMBS was therefore also analyzed with the Octet RED96 system with super streptavidin (SSA) biosensors in which data analysis using double reference subtraction accounts for nonspecific binding and minimizes the well-based and sensor variability. For the loading of the sensors, the protein needed to be biotinylated, but no alteration for the buffer conditions was required. The analyses with Octet provided an $S_{0.5}$ value of 83 ± 7 μ M for C6, obtained by fitting the data to a sigmoidal binding isotherm with saturable concentration dependence (Figure 2C, inset). For C6-3, SPR allowed the measurement of good concentration-dependent binding data, also with a sigmoidal binding curve, providing an $S_{0.5}$ value of 63 ± 3 μ M (Figure 2D).

Whereas C6-3 (and C5) showed a very weak noncompetitive inhibition, only affecting the V_{max} (Table 3), C6 showed uncompetitive inhibition and a decrease in both K_M and V_{max} (Table 2), indicating a preferential binding to the enzyme-substrate complex during catalysis rather than to the enzyme alone. It is difficult to predict binding sites for non-active site ligands, but uncompetitive inhibition customarily occurs by binding close to (still outside) the active site.⁴⁰ With the use of the pocket finder tool *fpocket* to identify binding sites adequate to accommodate stabilizing small-molecule compounds,⁴¹ the structure of the human HMBS

holoenzyme (PDB: 3ECR) revealed two relevant binding pockets other than the active site pocket (Figure 3A). However, computational protein-ligand docking suggested a favorable binding mode of both C6 (and C6-3; not shown) in only one of these pockets, close to the active site (Figure 3B). Consequent docking to the holoenzyme provided a top-score binding mode of C6 in which the hydroxyl and aldehyde oxygens of C6 interact with the guanidine group of Arg195, facilitating two hydrogen bonds, whereas the more hydrophobic part can interact with Leu238 and Val38 (Figure 3C). On the other hand, for C6-3, the oxygens that interact with Arg195 via hydrogen bonds are those in the nitro group (Figure 3D). The X-ray structure of an enzyme intermediate captured in the ES_2 state, with two PBG substrates bound to the covalently linked dipyrromethane (DPM) cofactor (PDB: 5M6R), allowed the prediction of the interaction of the PC candidates with intermediate states of HMBS other than the holoenzyme.⁴² Nevertheless, the analysis of this ES_2 -state structure revealed overlapping binding pockets as in the holoenzyme (Figures S5A and S5B). Subsequent docking to the ES_2 -state structure showed potential docking modes for the compounds with similar docking scores as for the holoenzyme-docked structures, with possible interactions with Val38 and Leu238.

Hit Compound C6 and Analog C6-3 Decrease ALA and PBG Excretion in *Hmbs*-Deficient Mice

In a second animal trial using *Hmbs*-deficient T1/T2^{-/-} mice, denoted trial T1/T2-B, we further investigated the PC potential of C5, C6, and C6-3 at higher concentration (20 mg/kg/day) than in trial T1/T2-A. The experimental setup was otherwise identical (Figure S2), with

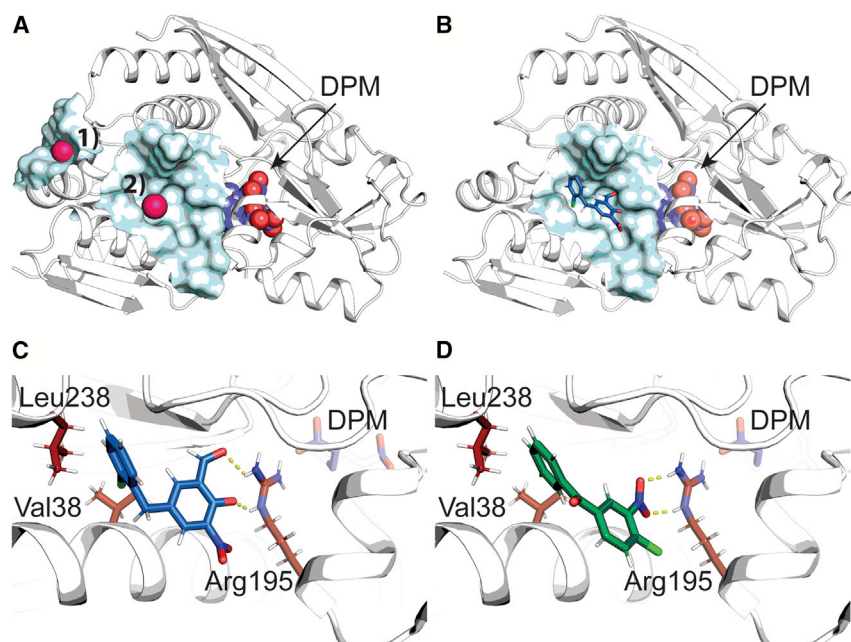


Figure 3. The Interaction of C6 and C6-3 with HMBS

(A) Potential binding pockets large enough to accommodate small-molecule compounds in HMBS. The structure of HMBS in the holoenzyme state (PDB: 3ECR) is shown in cartoon representation with the pockets (1 and 2) in pink spheres and cyan surface representation. The DPM cofactor is shown in purple and red spheres. (B) Top-score docked mode for C6, obtained for site 2 (blue sticks); see text for details. This pocket also scored highest for docking of C6-3. (C and D) Detailed view of the top-score docking mode of C6 (blue; C) and C6-3 (green; D) interacting with Arg195 in HMBS (PDB: 3ECR). In both panels, the DPM cofactor is located in the background, and Arg195, Val38, and Leu238 are denoted.

$n = 6$ in each treatment group and a control group ($n = 6$) receiving DMSO instead of compound. C5 was again included in the trial due to the overall good *in vitro* effects (Figure 1; Tables 1 and 2). The effect of compounds was, as in trial T1/T2-A, monitored by the measurement of urinary excretion of ALA and PBG. C5 did not perform as a potential PC of HMBS, as seen by the increase in ALA and PBG excretion by day 12 when mice were treated at 20 mg/kg/day of this compound, compared with the mice treated with a lower dose (Figures S3A and S3B) and to the controls (Figures 4A and 4B). This effect could be caused either by a possible porphyrinogenic effect³¹ or by a larger inhibitory effect *in vivo* than predicted *in vitro*. On the other hand, both C6 and C6-3 reduced the urinary ALA and PBG excretion and the latter to almost one-half of the value in the control group (Figures 4A and 4B). Furthermore, quantitative immunoblotting of liver tissue revealed an increase in steady-state levels of HMBS in the presence of all three compounds, with a significant increase only for C6 and C6-3 (Figure 4C). C5 was thus not included in further analyses of the effect of the compounds on hepatic HMBS activity and metabolite levels.

The effect of treatment with C6 and C6-3 on hepatic HMBS activity was measured in mice liver homogenates, and treatment with either hit compound resulted in significantly increased enzyme activity in the liver samples compared to the control group (Figure 4D). Furthermore, the relative concentrations of ALA and PBG were also determined in liver extracts, which were found to be decreased for the mice treated with C6 ($p < 0.05$ and $p = 0.053$, respectively, compared with control mice; Figures 4E and 4F).

DISCUSSION

Current AIP therapy investigations target the disease at a genetic level, including *HMBS* gene delivery, as well as RNAi therapy to decrease

ALAS1 expression.^{16–18} The first *HMBS* gene-delivery phase I clinical trial demonstrated that gene vector administration was safe, but a metabolic correction was not achieved at the doses tested.⁴³ Furthermore, heme is a central cofactor involved in diverse metabolic processes, and *ALAS1* is a highly regulated enzyme,⁴⁴ and downstream effects, such as energetic metabolism and long-term heme depletion, may be affected by RNAi therapy.^{16,45} In this work, we aim to target AIP at the protein level by developing a PC-based therapy. By achieving a structural equilibrium toward more native-like conformations, the consequences of misfolding mutations may be prevented.⁴⁶ We have, however, targeted the stabilization of the WT protein since most AIP patients have *HMBS* expression from one normal *HMBS* allele. We performed an experimental screening for compounds that stabilized recombinant WT-*HMBS* during thermal denaturation.^{47,48} Despite the high stability of *HMBS*,³⁴ we identified compounds that further stabilized WT-*HMBS*. We selected C5, C6, and an analog of the latter (C6-3) for *in vivo* studies based on a combination of *in vitro* and cell experiments that identified compounds that could increase the conformation stability and protect the enzyme activity. Furthermore, careful enzyme kinetic analysis with purified *HMBS* revealed weak inhibitory effects for these compounds. However, weak inhibitors have been shown to be good stabilizing PCs and activity enhancers *in vivo*.^{49,50} For C6, the results were particularly promising during the entire drug-discovery protocol, as it increased the steady-state levels of *HMBS* in cell studies (Figure 2A) and demonstrated potential as PCs in an animal trial at 20 mg/kg/day (Figure 4). We have previously shown that *HMBS*, which presents as a very stable enzyme as isolated (Figure 1A), loses conformational stability during catalysis or binding of the substrate.³⁴ Since both the inhibitory mechanism and docking of C6 and C6-3 support their binding to the substrate-enzyme complexes, the stabilizing effect of these compounds is expected to be even more relevant in cells and *in vivo* where the substrate is continuously available.

Accumulation of the precursors ALA and PBG plays important roles in the pathogenesis of AIP. ALA, in particular, has been implied to be the causative agent in acute neurovisceral attacks and neurological

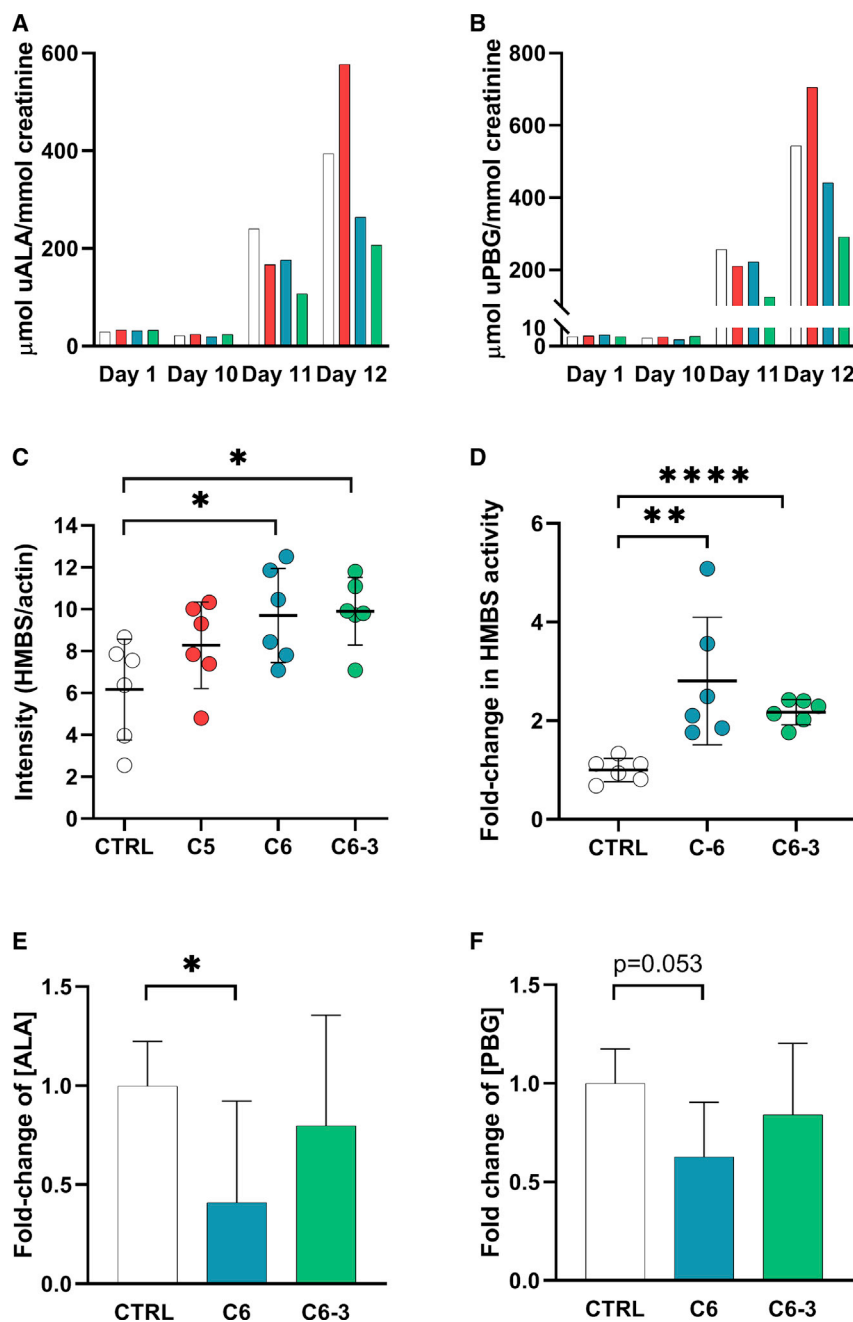


Figure 4. The Effect on ALA/PBG Excretion of the Hit Compound and Analog in *Hmbs*-Deficient Mice

Three groups of *Hmbs*-deficient $T1/T2^{-/-}$ mice ($n = 6$ in each group) were treated for 12 days with 20 mg/kg/day of C5, C6, or the analog C6-3, given orally. I.p. injection of phenobarbital was given on days 10–12 to induce the heme biosynthesis and thus, precipitation of biochemical acute attack. The control group was given 10% DMSO and likewise induced with phenobarbital. Urine was collected on days 1 and 10–12, and livers were harvested after sacrifice. (A and B) Bars represent porphyrin precursors ALA (A) and PBG (B) from C5 (red), C6 (blue), and C6-3 (green) treatment, measured in the urine (u) pooled for all mice from each group. The control group is shown in white. (C) HMBS protein levels measured in liver lysates by western blot quantification. Scatterplots with mean representing HMBS protein levels in mice livers treated with C5 (red), C6 (blue), and C6-3 (green). * $p < 0.05$ for differences with the corresponding control (10% DMSO without compound; white circles), calculated by unpaired two-tailed t test. Data are presented as mean \pm SD. (D) HMBS activity in liver lysates. Scatterplot with mean showing the hepatic HMBS activity after treatment with C6 (blue) and C6-3 (green). ** $p < 0.01$ and **** $p < 0.0001$ for differences with the corresponding control (10% DMSO without compound; white circles), calculated by unpaired two-tailed t test. Data are presented as mean \pm SD. (E and F) The relative concentrations of ALA (E) and PBG (F) were measured in liver tissue extracts after treatment with C6 (blue) and C6-3 (green). * $p < 0.05$ for differences with the corresponding control (10% DMSO without compound; white), calculated by unpaired two-tailed t test. Data are presented as mean \pm SD.

treated with either C6 or C6-3 before and during the challenge of heme biosynthesis with phenobarbital, resulted in an increase in steady-state levels of HMBS protein and activity, although a substantial decrease of porphyrin precursors in the liver was only measured for mice treated with C6 (Figures 4A, 4B, 4E, and 4F). Importantly, as the HMBS expressed in the mice model originates from the low-expressed normal allele, these hit compounds and notable C6 show potential to be developed into a large-spectrum PC medication that can operate on WT-HMBS *in vivo* and function for most AIP patients regardless of their mutation. Still, it is expected that the PCs would have a generalized stabilizing effect for many HMBS variants, especially those mutants

with increased instability compared with WT, such as R116W and V215E, among others.³⁴

symptoms.⁵¹ A decrease in ALA and PBG excretion in urine is a typical sign of successful treatment of patients with AIP symptoms, and patients with chronically high levels of these metabolites present normal ALA/PBG excretion following liver transplantation.^{52,53} In this work, we administered compounds to an *Hmbs*-deficient $T1/T2^{-/-}$ mouse model that exhibits residual expression of 30% from the low-expressed normal allele. After phenobarbital induction, the mice biochemically mimic an acute attack of AIP, showing increased urinary ALA and PBG levels.³³ *Hmbs*-deficient mice,

with increased instability compared with WT, such as R116W and V215E, among others.³⁴

HMBS is a dynamic protein where loops and possible interdomain flexibility accommodate the tetrapyrrole assembly with the enzyme,^{42,54,55} and intermediate complexes are being formed during the elongation. These intermediate states are present *in vivo* and also in the recombinant purified HMBS protein as an equilibrium of the states and may possess various formation rates with slightly different

conformations and stability.⁵⁶ In our work with WT-HMBS, we did not isolate the intermediates; however, PCs may be more effective toward specific intermediate states. Although the docking to the ES₂ structure did not reveal other favorable binding pockets, it cannot be ruled out that the intermediate reaction state and formation rate of HMBS will play a role in the binding of PCs. Furthermore, as HMBS is monomeric, and allostery has not been previously revealed, the sigmoidal binding curve for C6 and C6-3 might be explained by the presence of conformation ensembles in this enzyme.

At least two classes of PCs have been described: (1) active site-specific, also called classical PCs, and (2) non-active site PCs.^{49,57} The non-active site PCs hold the same stabilizing abilities as the active site-specific and in some cases, show allosteric activating function.^{58,59} Allosteric compounds may induce a more active conformation, as they can be bound to the target enzyme during catalysis without inhibiting activity.⁶⁰ The structure of HMBS clearly presents cavities that potentially can accommodate small molecular compounds, and the molecular docking supports the binding of the hit compounds at a pocket close to the active site, with a preferred binding to the substrate-bound HMBS compared to the free enzyme, due to proper orientation of Arg195 during catalysis. Arg195 is an important residue for HMBS activity^{61,62} that is also in direct contact with the cofactor.⁵⁵ Furthermore, Leu238 is identified as a hinge residue, and the compound hits may also stabilize a catalytically favorable conformation through this residue, perhaps with an allosteric effect. Despite the good conformity of the protein-ligand-binding modes, the docking structures must be interpreted with caution and ultimately be validated experimentally.

In conclusion, we provide proof of concept of PC therapy for AIP by *in vivo* experiments in *Hmbs*-deficient T1/T2^{-/-} mice, based on C6. Allosteric inhibition of HMBS by protoporphyrinogen and coproporphyrinogen has been implicated on the mechanism of acute attacks in variegate porphyria and hereditary coproporphyrinogen, and it is tempting to propose that this PC might be beneficial in the treatment of other acute porphyrias as well. Furthermore, this work adds to the recently discovered applicability of a PC-based therapy for congenital erythropoietic porphyria.²⁶ The expression of WT-HMBS from the normal allele, providing half-normal protein levels and activity in most AIP individuals, is advantageous in the development of PC therapy for AIP, regardless of mutation, as we show the possibility of an additionally increased stability and activity of the common WT-HMBS.^{24,28–30} In addition, it is assumed that the half-normal activity of HMBS is usually sufficient, and even a modest improvement of the enzymatic activity could be adequate in order to avoid phenotypic outcome,¹⁵ as has also been suggested for lysosomal storage enzymes.²⁵ PC therapy may also possess advantages compared with gene and RNAi therapies, such as orally administered treatment, resulting in no immunological reactions, and could be applied as both a prophylactic treatment and an intervention treatment during acute porphyria attacks. As many drugs are known to induce the rate-limiting ALAS,⁶⁴ the predicted way forward to a successful hit expansion and lead optimization, previous to structured toxicity analyses

for selection of the best drug candidate to enter clinical trials, should include analyses of porphyrinogenicity and derivatization of potential porphyrinogenic compounds into less toxic versions through medicinal chemistry.⁶³ In addition, further chemical efforts for rational hit-to-lead amplification and optimization, development of treatment protocols, and investigation of absorption, distribution, metabolism, and excretion (ADME)/pharmacokinetics (PK) parameters for the compounds will help to demonstrate the potential of PC therapy for AIP.

MATERIALS AND METHODS

Materials and Structure Validation of Hit Compounds

The MyriaScreen Diversity Collection (Sigma-Aldrich, St. Louis, Missouri), a small compound library was used to screen for hit compounds. It consists of 10,000 drug-like compounds at 2 mg/mL in 100% DMSO, with an average purity of 95%. The MW of the compounds varies from 220 to 547 Da. Hit compounds were subsequently obtained from MolPort (Vitas-M Chemical, Causeway Bay, Hong Kong, and Alinda Chemical, Moscow, Russia), dissolved in 100% DMSO, and stored at -20°C . The chemical structure of all hit compounds was confirmed by nuclear magnetic resonance (NMR).

Expression and Purification of HMBS Proteins

WT-HMBS were expressed and purified to apparent homogeneity, as previously described,³⁴ except for the enzyme used in the binding assays using the Octet RED96, which was expressed using a new construct with an N-terminal 6×histidine affinity tag and a tobacco etch virus (TEV) protease cleavage site, for which full-length HMBS was cloned into the pET-28a(+)-TEV vector and transformed into BL21 (DE3) cells for expression. Expression was performed using Terrific Broth medium with isopropyl β -D-1-thiogalactopyranoside (IPTG) induction for 16 h at 20°C with 220 rpm shaking. After harvesting, the cells were lysed with sonication, and purification was performed by Ni-nitrilotriacetic acid (NTA) affinity chromatography. The protein was eluted with 20 mM HEPES, 150 mM NaCl (pH 8), supplemented with 400 mM imidazole. The affinity tag was cleaved overnight and removed by Ni-NTA, and the protein was further purified by size-exclusion chromatography with a Superdex 75 10/300 GL or 16/60 PG column (GE Healthcare, Chicago, Illinois) in 20 mM HEPES, 150 mM NaCl (pH 8 or 8.0), respectively, and stored in aliquots in liquid N₂ until use.

High-Throughput Screening of Ligands Binding to HMBS

The thermal denaturation of recombinant WT-HMBS was monitored with the fluorescent probe SYPRO Orange (Thermo Fisher Scientific, Waltham, Massachusetts) in the search for stabilizing ligands among the 10,000 compounds from the MyriaScreen Diversity Collection, using DSF. The protocol for screening was as previously reported,²⁸ but in this work, we used a protein solution of 0.1 mg/mL HMBS in 20 mM Tris-HCl, 100 mM NaCl (pH 8.0), 5 × SYPRO Orange, and 0.04 mg/mL compound (averaged final concentration of 100 μM for all compounds in 2% DMSO). The samples were applied into 96-well PCR plates (Roche Diagnostics, Risch-Rotkreuz, Switzerland) and loaded into a Light Cycler 480 (Roche Diagnostics).

References with 2% DMSO without compounds were included on each plate. Unfolding curves were recorded with 0.2°C intervals with a scan rate of 2°C/min from 20°C to 95°C, and monitored at excitation (λ_{ex}) = 465 nm and emission (λ_{em}) = 610 nm. The experimental unfolding curves were normalized to fraction of unfolded protein (F_{u}) and smoothed using a Savitzky-Golay smoothing filter. The original hits were selected based on the T_{m} value and extracted from the fluorescence curves at the temperature where the scaled curves cross $y = 0.5$, but because of the complexity of the curves with several transitions, a qualitative inspection of each positive hit was also performed, using both the T_{m} and the dF/dT . Compounds that gave a positive $\Delta T_{\text{m}} \geq 1.5^\circ\text{C}$, providing a cutoff value of 3-fold $> \text{SD}$ for the T_{m} for DMSO controls in the screening, were defined as hit compounds and selected for further analyses.

Enzymatic Activity Assay of HMBS

The standard enzymatic activity of recombinant WT-HMBS was assayed in 50 mM HEPES (pH 8.2), 0.1% Triton-X, and 2% DMSO at 37°C, as reported.³⁴ Compounds were added at a concentration of 84 μM . The absorbance of uroporphyrinogen I was determined at 405 nm. The enzyme activity in the presence of compounds was normalized relative to DMSO control (relative activity). The effect of compounds on the stability of HMBS activity was assayed by preincubating the HMBS (4–5 μg) in 50 mM HEPES (pH 8.2), 84 μM compound, and 2% DMSO for 20 min at 70°C and then placed on ice for 5 min. The enzymatic activity at 37°C was subsequently measured as reported.³⁴ Controls without compound but with an equal concentration of DMSO were included. The remaining activity in the presence of compounds was normalized relative to DMSO control (relative activity). K_{M} and V_{max} were determined using an increasing concentration of PBG (3.125–1,000 μM), and the kinetic parameters were obtained by nonlinear fitting to Michaelis-Menten enzyme kinetics using GraphPad Prism version 8.2.0 for Windows (GraphPad Software, La Jolla, California, USA; <https://www.graphpad.com/>).

To assay the HMBS activity in liver lysates, the crude liver homogenates were passed through Zeba spin desalting columns (Thermo Fisher Scientific) using 50 mM HEPES (pH 8.2) as equilibration buffer. 25 μL filtrated homogenate (400–500 μg total protein) was added to 110 μL sample mix (50 mM HEPES [pH 8.2], 1% Triton X-100) and incubated for 10 min at 37°C before adding PBG (1 mM). The reaction was stopped after 1 h by adding ice-cooled 100% trichloroacetic acid (TCA) to a final concentration of 25%, incubated at room temperature (RT) for 10 min, and centrifuged at 10,000 g for 10 min. The absorption was measured in the supernatant at A_{409} with baseline correction at A_{380} using the NanoDrop 2000c spectrophotometer (Thermo Fisher Scientific). The activity of HMBS was expressed as relative activity in the compound-treated cell compared to DMSO controls. A blank sample was prepared for each homogenate. The unpaired t test (two-tailed) was performed using GraphPad Prism.

Limited Proteolysis by Trypsin

Limited proteolysis by trypsin was performed at 37°C in 20 mM HEPES, 150 mM NaCl, 2% DMSO (pH 8.2), with 0.15 $\mu\text{g}/\mu\text{L}$

HMBS in the absence (DMSO control) or presence of 84 μM compound and 2% DMSO. The proteolysis was initiated by adding 1 $\mu\text{g}/\text{mL}$ *N*-tosyl-L-phenylalanine chloromethyl ketone (TPCK)-treated trypsin (Sigma-Aldrich). After 30 min, aliquots were removed and transferred to Laemmli loading buffer containing 2 $\mu\text{g}/\text{mL}$ soybean trypsin inhibitor. Samples resolved by SDS-PAGE with 10% Mini-Protean TGX gels (Bio-Rad Laboratories, Hercules, California) were analyzed using the Image Lab software (Bio-Rad). The unpaired t test (two-tailed) was performed using GraphPad Prism.

Transfection of HepG2 Cells and Growth in the Presence of Compounds

The human hepatoma HepG2 cells were obtained from Leibniz-Institut DSMZ, Deutsche Sammlung von Mikroorganismen und Zellkulturen. Cells were maintained in RPMI 1640, GlutaMAX (Thermo Fisher Scientific) medium, supplemented with 10% heat-inactivated fetal bovine serum and 1% penicillin-streptomycin (Thermo Fisher Scientific) in a humidified incubator with 5% CO_2 at 37°C. HMBS cDNA was inserted into the pcDNA3.1(+) cloning vector (Thermo Fisher Scientific). The HepG2 cells were then transfected with the pcDNA3.1(+) vector containing HMBS using FuGENEHD Transfection Reagent (Promega, Madison, Wisconsin), according to the manufacturer's recommendations. Stably transfected clones were selected for resistance to the neomycin analog G418 (Thermo Fisher Scientific). WT-HMBS-transfected HepG2 cells (2×10^6) were seeded and grown for 22 h before compounds were added to final concentrations of 0, 40, 84, 120, and 168 μM in 2% DMSO. Cells were harvested after 24 h and analyzed as described below.

SPR

SPR experiments for the estimation of the concentration of compound at $S_{0.5}$ were performed using a Biacore T200 (GE Healthcare) instrument at 25°C. 150 $\mu\text{g}/\text{mL}$ WT-HMBS in 10 mM sodium acetate (pH 4.5) was immobilized onto a CM5-S sensor chip through amine-coupling chemistry and PBS containing 0.05% surfactant P20 as the running buffer, reaching immobilization levels $\sim 15,000$. The baseline was equilibrated for 1–2 h before C6 and C6-3 were assayed in a concentration-dependent manner (0–200 μM) using running buffer with 5% DMSO and 30 $\mu\text{L}/\text{min}$ flow rate. Contact and dissociation time was 60 s, with a final wash after 50% DMSO injection. Blank immobilization, solvent correction, and negative control (assay buffer) were included for the analysis of the sensorgrams using the Biacore T200 Evaluation software v2.0. The allosteric sigmoidal curve fitting was performed using GraphPad Prism.

Octet RED96

Octet RED96 system (FortéBio Biologics by Molecular Devices, San Jose, California) with super streptavidin (SSA) biosensors was used as an additional method for determining the binding affinity of C6. The loading of HMBS to the SSA sensors required biotinylation, which was carried out at room temperature, mixing 1.5 molar excess of *N*-hydroxysuccinimide (NHS)-ester biotinylation reagent (EZ-Link NHS-PEG4-Biotin; Thermo Fisher Scientific) to protein. After 30 min, excess of biotin was removed using Zeba spin desalting

columns (Thermo Fisher Scientific), and the gel filtration buffer was changed to reaction buffer, PBS-P+ (GE Healthcare), supplemented with 5% DMSO. Sensors were loaded with 5 $\mu\text{g}/\text{mL}$ of biotinylated HMBS, reaching 6 nm surface thickness. Triplicates for the concentration series of C6 were measured, and double-reference subtraction was applied for data analysis based on the steady-state kinetics with an equilibrium binding signal (R_{eq}) using ForteBio Data analysis 9.0. The allosteric sigmoidal curve fitting was performed using GraphPad Prism.

Animal Studies

The compound heterozygote *Hmbs*-deficient T1/T2^{-/-} mouse model³³ was utilized in the two sets of animal studies performed, T1/T2-A and T1/T2-B: (1) in the T1/T2-A study, mice (2–4 months old, 16–22 g) were given 10 mg/kg/day of either compound C5 or C6; (2) in the T1/T2-B study, mice (2–3 months old, 17–22 g) were treated with 20 mg/kg/day of hit compound C5 and C6 and analog C6-3. The mice in both groups were given phenobarbital (Gardenal) at 100 mg/kg through intraperitoneal (i.p.) injection on days 10–12 of the study. Urine from these mice was collected on day 1 before the start of treatment and each day of phenobarbital injection (days 10, 11, and 12). The protocol is presented in Figure S2.

Compounds were dissolved in 10% DMSO, and all studies included treatment groups with six mice in each, including a control group given only 10% DMSO. The compounds or DMSO alone were administered orally for 12 consecutive days, and the mice were sacrificed 30 min after the last dose of compound or phenobarbital. The mice were anaesthetized by i.p. injection of tribromoethanol (3 mg/kg), blood samples collected on EDTA by retro-orbital puncture, and livers harvested and flash frozen in liquid N₂ before storage at -80°C . Pooled urinary porphyrin precursor levels (ALA and PBG) were analyzed by sequential ion-exchange chromatography using the ALA/PBG by Column Test (Bio-Rad), according to the manufacturer's recommendations.

Study Approval

All animal experiments were performed according to procedures approved by the Bichat-Debré Ethics Committee. Animals were housed in a controlled environment with a 12-h light-dark photocycle, with free access to water and food.

Cell and Tissue Sampling

HepG2 cells were washed in ice-cold PBS before 10 min lysis on ice with cold radioimmunoprecipitation assay (RIPA) buffer (25 mM Tris-HCl, 150 mM NaCl, 1% Nonidet P-40 (NP-40), 1% sodium deoxycholate, 0.1% SDS [Cell Signaling Technologies, Danvers, Massachusetts] and cOMplete protease inhibitor cocktail [Roche Diagnostics]). Lysates were centrifuged (10,000 g, 4°C , 15 min), and supernatants were removed and stored at -80°C until further use. Frozen liver tissue was homogenized in 50 mM Tris-HCl (pH 7.4), 100 mM KCl, 1 mM DTT, 0.2 mM PMSF, 1 mM benzamidine, 1 mM EDTA, and 1 tablet/10 mL cOMplete ULTRA protease inhibitor cocktail (Roche Diagnostics) using TissueLyser II (QIAGEN,

Venlo, Netherlands). The extracts were clarified by centrifugation at 14,000 g for 20 min at 4°C , and supernatants were stored at -80°C .

Quantitative Detection of HMBS in Cell Lysate and Tissue by Immunoblot

Cell lysate samples (20 μg total protein) were separated by electrophoresis and subsequently transferred to a polyvinylidene difluoride (PVDF) transfer membrane (Bio-Rad). Membranes were blocked for 1 h at RT with 5% nonfat dry milk (Bio-Rad Laboratories) in Tris-buffered saline (TBS; 20 mM Tris-HCl, 140 mM NaCl [pH 7.4]), containing 0.1% Tween (0.1% TBS-T). Immunoblotting was carried out with 1:1,000 anti-HMBS primary antibody (Ab; H300; Santa Cruz Biotechnology, Dallas, Texas) in 0.1% TBS-T overnight at 4°C . Subsequently, the membranes were washed extensively in 0.1% TBS-T, followed by 1 h incubation at RT with horseradish peroxidase (HRP)-conjugated goat anti-rabbit immunoglobulin G (IgG) secondary Ab (Bio-Rad), 1:5,000 dilution. Anti-glyceraldehyde 3-phosphate dehydrogenase (GAPDH; Abcam, Cambridge, UK) was used as a loading control. Chemiluminescence of secondary Ab-HRP conjugates was elicited using Luminata Crescendo Western HRP Substrate (Merck Millipore, Burlington, Massachusetts), imaged with Gel Doc XR+ (Bio-Rad), and quantified using Image Lab software (Bio-Rad).

Liver homogenates (5 μg total protein/lane) were loaded onto 10% Mini-Protean TGX gels (Bio-Rad) and separated with Tris/glycine/SDS electrophoresis buffer (Bio-Rad). Trans-Blot Turbo Transfer Starter System (Bio-Rad) was used to transfer the proteins onto Immun-Blot low-fluorescence PVDF membranes (Bio-Rad). The membranes were then blocked with 1% TBS-T and 3% BSA for 1 h. HMBS was probed with 1:2,000 monoclonal mouse anti-HMBS (H-11; Santa Cruz Biotechnology), together with 1:1,000 rabbit anti-actin (Sigma-Aldrich), in 1% TBS-T, 3% BSA overnight, 4°C . Alexa Fluor 647-conjugated donkey anti-mouse and Alexa Fluor 488-conjugated donkey anti-rabbit (both Thermo Fisher Scientific) were used as secondary antibodies and incubated in 1:1,000 dilutions in 0.1% TBS-T for 1 h. Each step was followed by extensive washing with 0.1% TBS-T. Fluorescence detection was performed using G-Box Chemi-XRQ (Syngene Synoptics, Cambridge, UK) with filters UV06 and 705 nm for AF-488 and AF-647, respectively, and the band intensities of HMBS relative to the loading control (GAPDH) were determined using ImageJ.⁶⁵ Plotting and the unpaired two-tailed t test were performed using GraphPad Prism version 8.2.0.

Derivatization of C6

A similarity search of C6 was performed over the MolPort libraries (<https://www.molport.com/shop/index>) of commercially available compounds.⁶⁶ The libraries were downloaded from the ZINC database, and Tanimoto coefficients³⁸ to the query compounds were calculated for the 2D molecular similarity using OpenBabel and the ChemInf packages.³⁹ All compounds showing a Tanimoto coefficient of more than 70% to the query compounds were collected and clustered based on their pairwise similarity.

Protein-Ligand Docking

Identification of pockets on the surface of HMBS and possible binding sites were probed with fpocket⁴¹ using the structure with PDB: 3ECR⁵⁵ or 5M6R⁴² as input. Docking of C6 and C6-3 to the identified pockets was performed with Glide (Schrödinger, New York, NY)⁶⁷ using default settings for ligand and protein preparation, grid generation, and docking.

Determination of Metabolites in Liver Tissue Samples

One volume of homogenized liver tissue was mixed with two volumes of acetonitrile:MeOH (1:1, v/v) and centrifuged. High-performance liquid chromatography/tandem mass spectrometry (HPLC-MS/MS) was used to determine the concentration of ALA and PBG in the supernatants. Analyses of samples were conducted by the Bioanalytical Laboratory personnel at Enamine/Bienta (Bienta/Enamine Biology Services, Kiev, Ukraine; <http://bienta.net/>). The unpaired t tests (two-tailed) were performed using GraphPad Prism version 8.2.0.

Statistics

Results are presented as mean \pm SD. Statistical comparisons were done using unpaired two-tailed t test, and statistical significance was defined as $p < 0.05$ or lower, as specified in the text. All statistical analyses and plotting of data were performed in GraphPad Prism 8.2.0.

SUPPLEMENTAL INFORMATION

Supplemental Information can be found online at <https://doi.org/10.1016/j.ymthe.2019.11.010>.

AUTHOR CONTRIBUTIONS

Conceptualization, A.M.; Methodology, C.S., H.J.B., J.U., K.T., and M.V.; Investigation, C.S., H.J.B., J.P.K., J.U., K.T., M.V., S. Simonin, and P.L.; Resources, A.M., C.S., H.J.B., K.T., M.V., and S. Sandberg; Writing—Original Draft, H.J.B.; Writing—Review and Editing, A.M., C.S., H.J.B., K.T., M.V., and S. Sandberg; Visualization, H.J.B.; Supervision, A.M. and S. Sandberg; Project Administration, A.M.; Funding Acquisition, A.M. and S. Sandberg.

CONFLICTS OF INTEREST

The authors are filing a patent application for the potential of C6 and C6-3 for development of a treatment for acute intermittent porphyria.

ACKNOWLEDGMENTS

We are very grateful to Ming Ying for expert help with immunoblot and immunoquantifications. The authors thank the K. G. Jebsen Foundation, Western Norwegian Regional Health Authorities (grant 912246), Norwegian Research Council for grants FRIMEDBIO 261826/F20, BIOTEK2021 285295, Norwegian NMR Platform, NNP 226244/F50, and infrastructure project NOR-OPENSREEN (245922/F50).

REFERENCES

- Karim, Z., Lyoumi, S., Nicolas, G., Deybach, J.C., Gouya, L., and Puy, H. (2015). Porphyrias: A 2015 update. *Clin. Res. Hepatol. Gastroenterol.* 39, 412–425.
- Harper, P., and Sardh, E. (2014). Management of acute intermittent porphyria. *Expert Opin. Orphan Drugs* 2, 349–368.
- Lenglet, H., Schmitt, C., Grange, T., Manceau, H., Karboul, N., Bouchet-Crivat, F., Robreau, A.M., Nicolas, G., Lamoril, J., Simonin, S., et al. (2018). From a dominant to an oligogenic model of inheritance with environmental modifiers in acute intermittent porphyria. *Hum. Mol. Genet.* 27, 1164–1173.
- Chen, B., Solis-Villa, C., Hakenberg, J., Qiao, W., Srinivasan, R.R., Yasuda, M., Balwani, M., Doheny, D., Peter, I., Chen, R., and Desnick, R.J. (2016). Acute Intermittent Porphyria: Predicted Pathogenicity of HMBS Variants Indicates Extremely Low Penetrance of the Autosomal Dominant Disease. *Hum. Mutat.* 37, 1215–1222.
- Bissell, D.M., Lai, J.C., Meister, R.K., and Blanc, P.D. (2015). Role of delta-aminolevulinic acid in the symptoms of acute porphyria. *Am. J. Med.* 128, 313–317.
- Unzu, C., Sampedro, A., Sardh, E., Mauleón, I., Enriquez de Salamanca, R., Prieto, J., Salido, E., Harper, P., and Fontanellas, A. (2012). Renal failure affects the enzymatic activities of the three first steps in hepatic heme biosynthesis in the acute intermittent porphyria mouse. *PLoS ONE* 7, e32978.
- Shoolingin-Jordan, P., and McNeill, L. (2003). Molecular changes in porphobilinogen deaminase in AIP *Porphyrias and Porphyrias* (Physiological Research), pp. 1S–33S.
- Pischik, E., and Kauppinen, R. (2015). An update of clinical management of acute intermittent porphyria. *Appl. Clin. Genet.* 8, 201–214.
- Besur, S., Schmeltzer, P., and Bonkovsky, H.L. (2015). Acute Porphyrias. *J. Emerg. Med.* 49, 305–312.
- Baravelli, C.M., Sandberg, S., Aarsand, A.K., Nilsen, R.M., and Tollånes, M.C. (2017). Acute hepatic porphyria and cancer risk: a nationwide cohort study. *J. Intern. Med.* 282, 229–240.
- Pallet, N., Mami, I., Schmitt, C., Karim, Z., François, A., Rabant, M., Nochy, D., Gouya, L., Deybach, J.C., Xu-Dubois, Y., et al. (2015). High prevalence of and potential mechanisms for chronic kidney disease in patients with acute intermittent porphyria. *Kidney Int.* 88, 386–395.
- Bonkovsky, H.L., Healey, J.F., Lourie, A.N., and Geron, G.G. (1991). Intravenous heme-albumin in acute intermittent porphyria: evidence for repletion of hepatic hemo-proteins and regulatory heme pools. *Am. J. Gastroenterol.* 86, 1050–1056.
- Schmitt, C., Lenglet, H., Yu, A., Delaby, C., Benecke, A., Lefebvre, T., Letteron, P., Paradis, V., Wahlin, S., Sandberg, S., et al. (2018). Recurrent attacks of acute hepatic porphyria: major role of the chronic inflammatory response in the liver. *J. Intern. Med.* 284, 78–91.
- Wahlin, S., Harper, P., Sardh, E., Andersson, C., Andersson, D.E., and Ericzon, B.G. (2010). Combined liver and kidney transplantation in acute intermittent porphyria. *Transpl. Int.* 23, e18–e21.
- Yin, Z., Wahlin, S., Ellis, E.C., Harper, P., Ericzon, B.G., and Nowak, G. (2014). Hepatocyte transplantation ameliorates the metabolic abnormality in a mouse model of acute intermittent porphyria. *Cell Transplant.* 23, 1153–1162.
- D'Avola, D., López-Franco, E., Sangro, B., Pañeda, A., Grossios, N., Gil-Farina, I., Benito, A., Twisk, J., Paz, M., Ruiz, J., et al. (2016). Phase I open label liver-directed gene therapy clinical trial for acute intermittent porphyria. *J. Hepatol.* 65, 776–783.
- Chan, A., Liebow, A., Yasuda, M., Gan, L., Racie, T., Maier, M., Kuchimanchi, S., Foster, D., Milstein, S., Charisse, K., et al. (2015). Preclinical Development of a Subcutaneous ALAS1 RNAi Therapeutic for Treatment of Hepatic Porphyrias Using Circulating RNA Quantification. *Mol. Ther. Nucleic Acids* 4, e263.
- Jiang, L., Berraondo, P., Jericó, D., Guey, L.T., Sampedro, A., Frassetto, A., Benenato, K.E., Burke, K., Santamaria, E., Alegre, M., et al. (2018). Systemic messenger RNA as an etiological treatment for acute intermittent porphyria. *Nat. Med.* 24, 1899–1909.
- Conn, P.M., Spicer, T.P., Scampavia, L., and Janovick, J.A. (2015). Assay strategies for identification of therapeutic leads that target protein trafficking. *Trends Pharmacol. Sci.* 36, 498–505.

20. Martinez, A., Calvo, A.C., Teigen, K., and Pey, A.L. (2008). Rescuing proteins of low kinetic stability by chaperones and natural ligands phenylketonuria, a case study. *Prog. Mol. Biol. Transl. Sci.* 83, 89–134.
21. Leidenheimer, N.J., and Ryder, K.G. (2014). Pharmacological chaperoning: a primer on mechanism and pharmacology. *Pharmacol. Res.* 83, 10–19.
22. Gomes, C.M. (2012). Protein misfolding in disease and small molecule therapies. *Curr. Top. Med. Chem.* 12, 2460–2469.
23. Van Goor, F., Hadida, S., Grootenhuys, P.D., Burton, B., Stack, J.H., Straley, K.S., Decker, C.J., Miller, M., McCartney, J., Olson, E.R., et al. (2011). Correction of the F508del-CFTR protein processing defect in vitro by the investigational drug VX-809. *Proc. Natl. Acad. Sci. USA* 108, 18843–18848.
24. Pey, A.L., Ying, M., Cremades, N., Velazquez-Campoy, A., Scherer, T., Thöny, B., Sancho, J., and Martinez, A. (2008). Identification of pharmacological chaperones as potential therapeutic agents to treat phenylketonuria. *J. Clin. Invest.* 118, 2858–2867.
25. Parenti, G., Andria, G., and Valenzano, K.J. (2015). Pharmacological Chaperone Therapy: Preclinical Development, Clinical Translation, and Prospects for the Treatment of Lysosomal Storage Disorders. *Mol. Ther.* 23, 1138–1148.
26. Urquiza, P., Lain, A., Sanz-Parra, A., Moreno, J., Bernardo-Seisdedos, G., Dubus, P., González, E., Gutiérrez-de-Juan, V., García, S., Eraña, H., et al. (2018). Repurposing ciclopirox as a pharmacological chaperone in a model of congenital erythropoietic porphyria. *Sci. Transl. Med.* 10, eaat7467.
27. Badminton, M.N., and Elder, G.H. (2005). Molecular mechanisms of dominant expression in porphyria. *J. Inherit. Metab. Dis.* 28, 277–286.
28. Jorge-Finnigan, A., Brasil, S., Underhaug, J., Ruiz-Sala, P., Merinero, B., Banerjee, R., Desviat, L.R., Ugarte, M., Martínez, A., and Pérez, B. (2013). Pharmacological chaperones as a potential therapeutic option in methylmalonic aciduria cblB type. *Hum. Mol. Genet.* 22, 3680–3689.
29. Kornhaber, G.J., Tropak, M.B., Maegawa, G.H., Tuske, S.J., Coales, S.J., Mahuran, D.J., and Hamuro, Y. (2008). Isogagomine induced stabilization of glucocerebrosidase. *ChemBioChem* 9, 2643–2649.
30. Scavelli, R., Ding, Z., Blau, N., Haavik, J., Martínez, A., and Thöny, B. (2005). Stimulation of hepatic phenylalanine hydroxylase activity but not Pah-mRNA expression upon oral loading of tetrahydrobiopterin in normal mice. *Mol. Genet. Metab.* 86 (Suppl 1), S153–S155.
31. Roveri, G., Nascimbeni, F., Rocchi, E., and Ventura, P. (2014). Drugs and acute porphyrias: reasons for a hazardous relationship. *Postgrad. Med.* 126, 108–120.
32. James, M.F., and Hift, R.J. (2000). Porphyrias. *Br. J. Anaesth.* 85, 143–153.
33. Lindberg, R.L., Porcher, C., Grandchamp, B., Ledermann, B., Bürki, K., Brandner, S., Aguzzi, A., and Meyer, U.A. (1996). Porphobilinogen deaminase deficiency in mice causes a neuropathy resembling that of human hepatic porphyria. *Nat. Genet.* 12, 195–199.
34. Bustad, H.J., Vorland, M., Rønneseth, E., Sandberg, S., Martínez, A., and Toska, K. (2013). Conformational stability and activity analysis of two hydroxymethylbilane synthase mutants, K132N and V215E, with different phenotypic association with acute intermittent porphyria. *Biosci. Rep.* 33, 33.
35. Niesen, F.H., Berglund, H., and Vedadi, M. (2007). The use of differential scanning fluorimetry to detect ligand interactions that promote protein stability. *Nat. Protoc.* 2, 2212–2221.
36. Ghosh, K., and Dill, K. (2010). Cellular proteomes have broad distributions of protein stability. *Biophys. J.* 99, 3996–4002.
37. Baell, J.B., and Holloway, G.A. (2010). New substructure filters for removal of pan assay interference compounds (PAINS) from screening libraries and for their exclusion in bioassays. *J. Med. Chem.* 53, 2719–2740.
38. Bender, A., and Glen, R.C. (2004). Molecular similarity: a key technique in molecular informatics. *Org. Biomol. Chem.* 2, 3204–3218.
39. O'Boyle, N.M., Banck, M., James, C.A., Morley, C., Vandermeersch, T., and Hutchison, G.R. (2011). Open Babel: An open chemical toolbox. *J. Cheminform.* 3, 33.
40. Sintchak, M.D., and Nimmesgern, E. (2000). The structure of inosine 5'-monophosphate dehydrogenase and the design of novel inhibitors. *Immunopharmacology* 47, 163–184.
41. Le Guilloux, V., Schmidtke, P., and Tuffery, P. (2009). Fpocket: an open source platform for ligand pocket detection. *BMC Bioinformatics* 10, 168.
42. Pluta, P., Roversi, P., Bernardo-Seisdedos, G., Rojas, A.L., Cooper, J.B., Gu, S., Pickersgill, R.W., and Millet, O. (2018). Structural basis of pyrrole polymerization in human porphobilinogen deaminase. *Biochim. Biophys. Acta, Gen. Subj.* 1862, 1948–1955.
43. Brunetti-Pierri, N., and Newsome, P.N. (2016). AAV-mediated liver-directed gene therapy for Acute Intermittent Porphyria: It is safe but is it effective? *J. Hepatol.* 65, 666–667.
44. Ajioka, R.S., Phillips, J.D., and Kushner, J.P. (2006). Biosynthesis of heme in mammals. *Biochim. Biophys. Acta* 1763, 723–736.
45. Hamedan, C., Schmitt, C., Laafi, J., Gueguen, N., Desquiret-Dumas, V., Lenglet, H., Karim, Z., Gouya, L., Deybach, J.C., Simard, G., et al. (2015). Mitochondrial energetic defects in muscle and brain of a Hmbs^{-/-} mouse model of acute intermittent porphyria. *Hum. Mol. Genet.* 24, 5015–5023.
46. Fan, J.Q. (2003). A contradictory treatment for lysosomal storage disorders: inhibitors enhance mutant enzyme activity. *Trends Pharmacol. Sci.* 24, 355–360.
47. Underhaug, J., Aubi, O., and Martínez, A. (2012). Phenylalanine hydroxylase misfolding and pharmacological chaperones. *Curr. Top. Med. Chem.* 12, 2534–2545.
48. Convertino, M., Das, J., and Dokholyan, N.V. (2016). Pharmacological Chaperones: Design and Development of New Therapeutic Strategies for the Treatment of Conformational Diseases. *ACS Chem. Biol.* 11, 1471–1489.
49. Fan, J.Q. (2008). A counterintuitive approach to treat enzyme deficiencies: use of enzyme inhibitors for restoring mutant enzyme activity. *Biol. Chem.* 389, 1–11.
50. Suzuki, H., Ohto, U., Higaki, K., Mena-Barragán, T., Aguilar-Moncayo, M., Ortiz Mellet, C., Nanba, E., García Fernández, J.M., Suzuki, Y., and Shimizu, T. (2014). Structural basis of pharmacological chaperoning for human β -galactosidase. *J. Biol. Chem.* 289, 14560–14568.
51. Simon, N.G., and Herkes, G.K. (2011). The neurologic manifestations of the acute porphyrias. *J. Clin. Neurosci.* 18, 1147–1153.
52. Soonawalla, Z.F., Orug, T., Badminton, M.N., Elder, G.H., Rhodes, J.M., Bramhall, S.R., and Elias, E. (2004). Liver transplantation as a cure for acute intermittent porphyria. *Lancet* 363, 705–706.
53. Dar, F.S., Asai, K., Haque, A.R., Cherian, T., Rela, M., and Heaton, N. (2010). Liver transplantation for acute intermittent porphyria: a viable treatment? *HBPD INT* 9, 93–96.
54. Louie, G.V., Brownlie, P.D., Lambert, R., Cooper, J.B., Blundell, T.L., Wood, S.P., Warren, M.J., Woodcock, S.C., and Jordan, P.M. (1992). Structure of porphobilinogen deaminase reveals a flexible multidomain polymerase with a single catalytic site. *Nature* 359, 33–39.
55. Song, G., Li, Y., Cheng, C., Zhao, Y., Gao, A., Zhang, R., Joachimiak, A., Shaw, N., and Liu, Z.J. (2009). Structural insight into acute intermittent porphyria. *FASEB J.* 23, 396–404.
56. Noriega, G., Mattei, G., Batlle, A., and Juknat, A.A. (2002). Rat kidney porphobilinogen deaminase kinetics. Detection of enzyme-substrate complexes. *Int. J. Biochem. Cell Biol.* 34, 1230–1240.
57. Yue, W.W. (2016). From structural biology to designing therapy for inborn errors of metabolism. *J. Inherit. Metab. Dis.* 39, 489–498.
58. Nussinov, R., and Tsai, C.J. (2013). Allostery in disease and in drug discovery. *Cell* 153, 293–305.
59. Jung, O., Patnaik, S., Marugan, J., Sidransky, E., and Westbroek, W. (2016). Progress and potential of non-inhibitory small molecule chaperones for the treatment of Gaucher disease and its implications for Parkinson disease. *Expert Rev. Proteomics* 13, 471–479.
60. Porto, C., Ferrara, M.C., Meli, M., Acampora, E., Avolio, V., Rosa, M., Cobucci-Ponzano, B., Colombo, G., Moracci, M., Andria, G., and Parenti, G. (2012).

- Pharmacological enhancement of alpha-glucosidase by the allosteric chaperone N-acetylcysteine. *Mol. Ther.* 20, 2201–2211.
61. Kauppinen, R., Mustajoki, S., Pihlaja, H., Peltonen, L., and Mustajoki, P. (1995). Acute intermittent porphyria in Finland: 19 mutations in the porphobilinogen deaminase gene. *Hum. Mol. Genet.* 4, 215–222.
 62. Pischik, E., Mehtälä, S., and Kauppinen, R. (2005). Nine mutations including three novel mutations among Russian patients with acute intermittent porphyria. *Hum. Mutat.* 26, 496.
 63. Meissner, P., Adams, P., and Kirsch, R. (1993). Allosteric inhibition of human lymphoblast and purified porphobilinogen deaminase by protoporphyrinogen and coproporphyrinogen. A possible mechanism for the acute attack of variegate porphyria. *J. Clin. Invest.* 91, 1436–1444.
 64. Hift, R.J., Thunell, S., and Brun, A. (2011). Drugs in porphyria: From observation to a modern algorithm-based system for the prediction of porphyrogenicity. *Pharmacol. Ther.* 132, 158–169.
 65. Schneider, C.A., Rasband, W.S., and Eliceiri, K.W. (2012). NIH Image to ImageJ: 25 years of image analysis. *Nat. Methods* 9, 671–675.
 66. Irwin, J.J., Sterling, T., Mysinger, M.M., Bolstad, E.S., and Coleman, R.G. (2012). ZINC: a free tool to discover chemistry for biology. *J. Chem. Inf. Model.* 52, 1757–1768.
 67. Friesner, R.A., Banks, J.L., Murphy, R.B., Halgren, T.A., Klicic, J.J., Mainz, D.T., Repasky, M.P., Knoll, E.H., Shelley, M., Perry, J.K., et al. (2004). Glide: a new approach for rapid, accurate docking and scoring. 1. Method and assessment of docking accuracy. *J. Med. Chem.* 47, 1739–1749.

YMTHE, Volume 28

Supplemental Information

A Pharmacological Chaperone Therapy

for Acute Intermittent Porphyria

Helene J. Bustad, Karen Toska, Caroline Schmitt, Marta Vorland, Lars Skjærven, Juha P. Kallio, Sylvie Simonin, Philippe Letteron, Jarl Underhaug, Sverre Sandberg, and Aurora Martinez

Supplemental data

Table S1. Overview of the 13 primary hit compounds.

ID	IUPAC name	logP ^a	Mw
C4	(2Z)-3-[(4-Bromophenyl)amino]-2-[[4-bromophenyl)amino](2-furyl)methyl}acrylaldehyde	5.26	476.17
C5	2-methoxy-N-[(phenylcarbamothioyl)amino]acetamide	-0.40	239.3
C6	5-[(2-chlorophenyl)methyl]-2-hydroxy-3-nitrobenzaldehyde	4.36	291.69
C8	6-Amino-4-(3-chlorophenyl)-3-methyl-7-(4-nitrophenyl)-4,7-dihydro[1,2]oxazolo[5,4-b]pyridine-5-carbonitrile	3.09	407.82
C9	9,10-Dimethoxy-8-phenyl-5,8-dihydro-6H-[1,3]dioxolo[4,5-g]isoquinolino[3,2-a]isoquinoline	4.88	413.47
C11	(E)-2-[4-(2-bromophenyl)thiazol-2-yl]-3-(2-thienyl)prop-2-enenitrile	4.18	373.3
C12	6-(4-chloro-3-nitro-phenyl)-2,3,9,9-tetramethyl-6,8,10,11-tetrahydro-5H-benzo[b][1,4]benzodiazepin-7-one	4.81	425.91
C15	4-[4-(1,3-Benzodioxol-5-yl)-1H-pyrazol-3-yl]-6-propyl-1,3-benzenediol	3.70	338.36
C16	1-(4-Chlorophenyl)-3-(3-fluoro-4-methylphenyl)urea	4.69	278.71
C17	N-(2,5-Dimethylphenyl)-2-(4-oxo-3(4H)-quinazolinyl)acetamide	1.77	307.35
C19	4-Acetylphenyl (4-chlorophenyl)carbamate	3.50	289.72
C23	1-(4-Methoxyphenoxy)-7-methyl-3-nitrobenzo[b,f][1,4]oxazepin-11(10H)-one	3.50	392.37
C24	2-[(1,3-Benzodioxol-5-ylamino)methyl]-4-bromophenol	4.27	322.16

^aLogP describes the logarithm of the partition coefficient between n-octanol and water $\log(c_{\text{octanol}}/c_{\text{water}})$, calculated from the chemical formula. The values are provided by Sigma-Aldrich.

Figure S1. Effect of hit compound C5, C11 and C17 on HMBS levels in HepG2 cells. The western blots show the immunodetection of HMBS and GAPDH (loading control) in lysates from WT-HMBS transfected HepG2 cells after treatment with C5, C11 or C17 at the indicated concentrations. See main text for further details. Std, molecular weight standards at 40 kDa and 50 kDa.

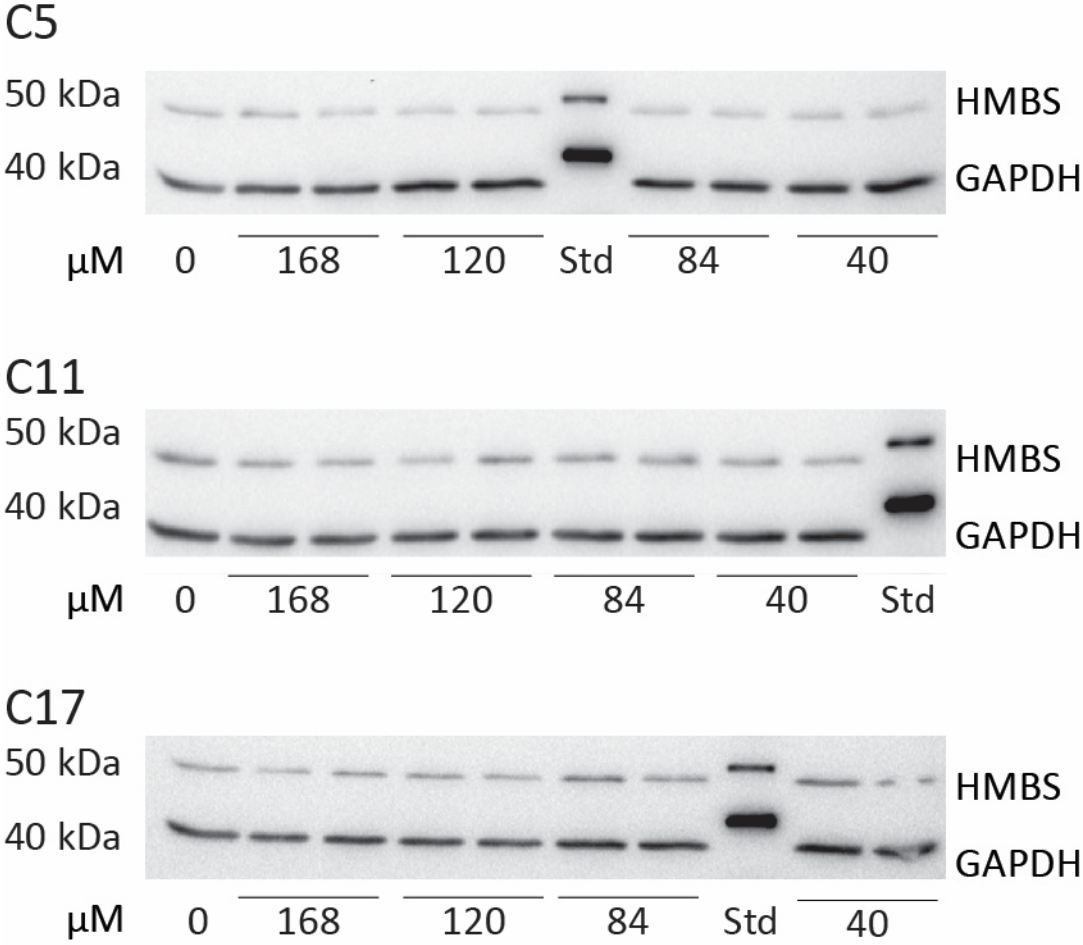


Figure S2: Schematic protocol followed in mice trials. Female compound heterozygote *Hmbs*-deficient T1/T2^{-/-} mice (n=6 per group) were kept on normal diet and given 10 or 20 mg/kg/day (trial T1/T2-A and T1/T2-B, respectively) of either hit compounds or DMSO, by oral gavage, for 12 consecutive days. Biochemical acute attack was induced by intraperitoneal injection of phenobarbital days 10–12. Urine was collected on day 1 and 10–12, and blood samples were collected before sacrifice. Livers were harvested after sacrifice.

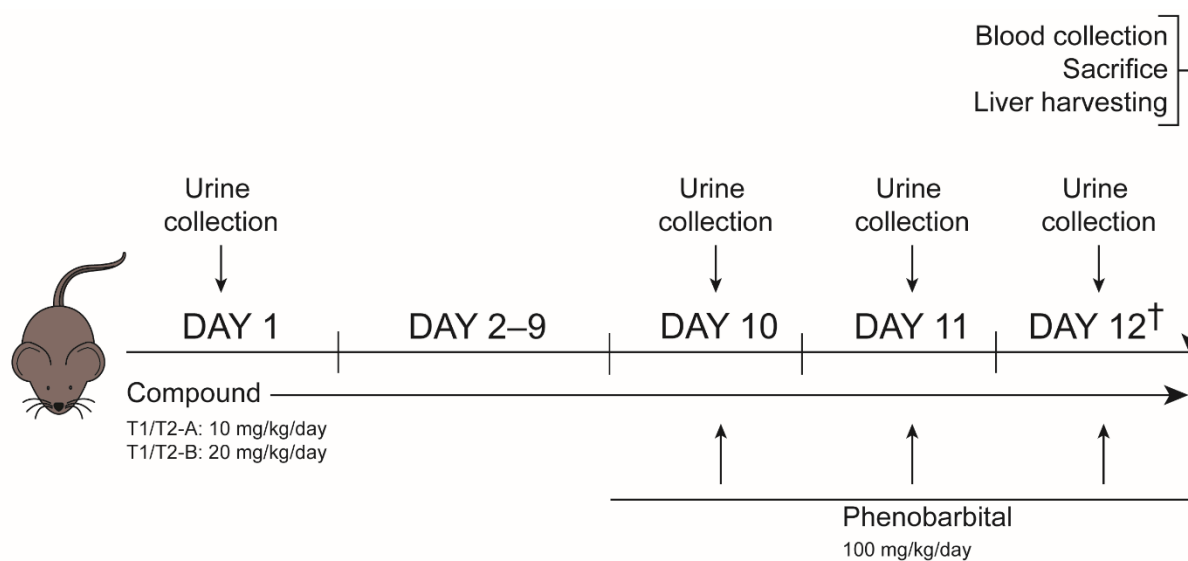


Figure S3: Effect of the hit compounds C5 and C6 in *Hmbs*^{-/-} mice (trial T1/T2-A). Two groups of *Hmbs* T1/T2^{-/-} mice (n=6 in each group) were orally treated for 12 days with 10 mg/kg/day of C5 and C6. On day 10, 11 and 12 they were induced by phenobarbital. A control group (n=6) was given 10% DMSO, and likewise induced with phenobarbital. On days 1 and 10–12 urine was collected and pooled from each group before measurement. See Fig. S2 for schematic presentation of treatment protocol. **(A, B)** Bars represent porphyrin precursor **(A)** ALA and **(B)** PBG in urine from control group (grey), C5 (red) and C6 (blue).

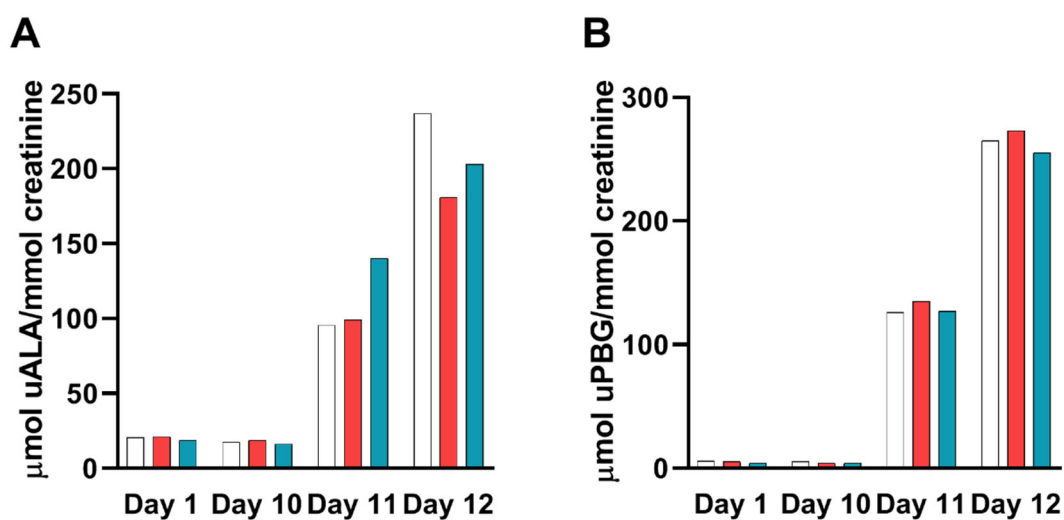


Figure S4: Concentration-dependent surface plasmon resonance. (A,B) Representative original sensorgrams with the increase of concentration of either C6 (A) or C6-3 (B), up to 200 μ M, shown in corresponding decrease in color intensity.

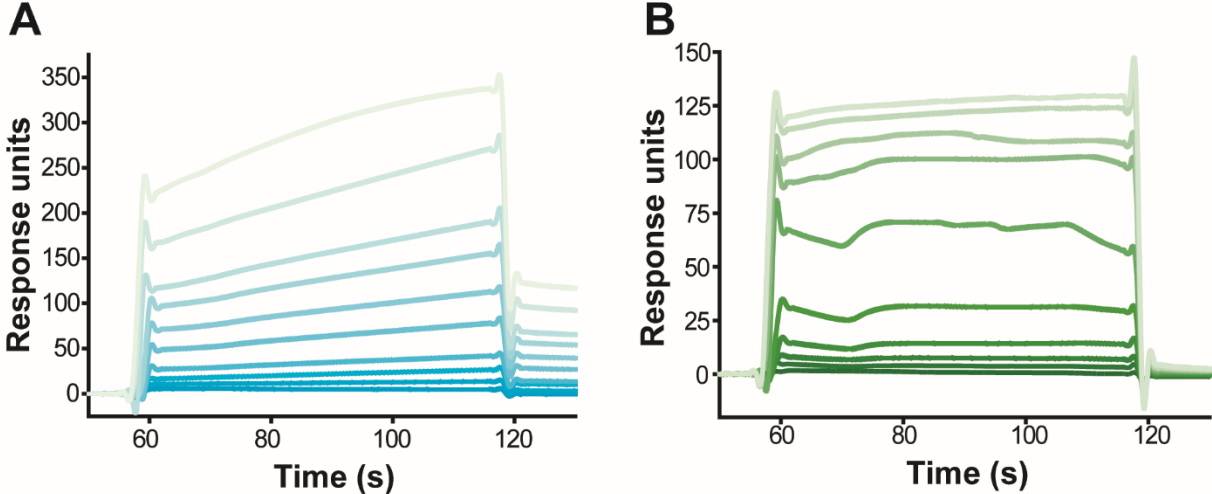


Figure S5: The interaction of C6 and C6-3 with HMBS reaction intermediate ES₂. The structure of HMBS in the ES₂ state (PDB ID: 5M6R) provided overlapping pockets as in the holoenzyme, and is shown in cartoon representation with cyan surface representing the pockets. The DPM cofactor with two additional substrates are visualized in green and red spheres. (A,B) Top-score docking modes for C6 (blue and orange sticks; A) and C6-3 (pink and yellow sticks; B).

